Vol. 3, No. 3, pp. 313-323, (September 2022)
DOI: 10.21608/aujes.2022.142530.1070
Aswan University Journal of Environmental Studies (AUJES)
Online ISSN: 2735-4237, Print ISSN: 2735-4229
Journal homepage: https://aujes.journals.ekb.eg/ E-mail: AUJES@aswu.edu.eg
Original research

Structural and Morphological Features of Hydroxyapatite Nanoparticles from Different Calcium Resources

Safaa El Nahas[1], Adilla E. Mohamed[2], Randa R. Ahmed*[2]
[1]*Chemistry Department, Faculty of Science, South Valley University, Qena 83523, Egypt*
[2]*Chemistry Department, Faculty of Science, Aswan University, Sahary 81528, Egypt*

Received: 25/6/2022 Accepted: 6/7/2022

Abstract:

The shape of the growing crystals during creation of nano-hydroxyapatite materials is influenced critically by the source of calcium salt. Hydroxyapatite may be utilized in a wide range of applications due to its various morphological structures. Four samples of nano-hydroxyapatite were synthesized using inexpensive and readily available calcium salt sources. Samples have also been characterized and analyzed via XRD, FTIR, SEM, TG, and S_{BET} methods. The weight losses for the HAp samples investigated varied from 1% to 3%, indicating that they were all thermally stable. During the interaction of various calcium ions with concentrated phosphoric acid, the presence of various anions throughout the preparation process acts as a structure shaping agent. Coral reef-shape, Sticks, nano-sheet and cotton-shape morphological structures resulted according to SEM analyses. All tested materials showed a high surface area following the order HA-Cl (162.73 m^2/g) > HA-OH (136.32 m^2/g) > HA-AC (135.27 m^2/g) > HA-NO_3 (115.98 m^2/g). The hydroxyapatites studied have crystallite sizes ranging from 14.85 to 25.72 nm, putting them on the Nano scale. Tested hydroxyapatite materials were effectively utilized to remove contaminants such as Fe^{3+} and Mn^{2+} from water with efficiencies of up to 95%. The total cost ranged from 258-386 EGP/100g (13.02-19.47) €/100g, including electricity costs.

Keywords: Nano-hydroxyapatite, Adsorption, Water treatment, Polluti

1- Introduction

Hydroxyapatite (HAp) is one of the most useful calcium phosphate compounds (Fihri et al., 2017). Hydroxyapatite is similar to bone tissue in terms of chemical composition and physical properties. HAp is biocompatible with the human body and has bioactive properties. As a result, a lot of work has gone into developing, identifying, and utilizing HAp in the biomedical applications, especially bone tissue engineering (Dileepkumar et al., 2022).

Corresponding author*: E-mail address: reno.roshdy92@gmail.com

Hydroxyapatite (HAp) is the major mineral structure of bone and teeth, as well as it is the key ingredient required for their hardness and strength. Its chemical formula is Ca_{10} $(PO_4)_6(OH)$ (Ibrahim et al., 2020). Furthermore, hydroxyapatite nanomaterial (HAp) is a perfect transporter for the regulated release of drugs since it is the most stable calcium phosphate precursor (Munir et al., 2022). Furthermore, HApis the most thermally stable crystalline form of Ca/P in physiological fluid, that closest to the mineral component of bones (Sadat-Shojai et al., 2013).

The physicochemical characteristics and morphology of hydroxyapatite (HA) varied depending on the production methods. The two main ways for getting hydroxyapatite are inorganic synthesis and apatite (HA) from natural sources. The transfer of infection is a problem in natural hydroxyapatite (HA) when proper preparation is not followed to remove all proteins. Synthetic hydroxyapatite is prepared by solid-state processes, co-precipitation, the sol-gel process, micro emulsion, and the hydrothermal approach (Bouyegh et al., 2021). For its distinct ions structure, the HAp is a dielectric material that increases the electrical characteristics of its mixtures. Its electronic properties vary depending on a variety of factors including: preparation techniques, calcium/phosphorous (Ca/P) ratios, nonstoichiometric, defects, crystallite size, and the possibility of a surface atmospheric reaction. In order to explore the electrical structure of synthetic HAp synthesized from various anionic precursors, the atomic and structural properties of synthetic HA must be investigated (Sundarabharathi et al., 2019). The current global market for HAp is worth USD 2.2 billion, with a forecast of USD 3.3 billion by 2025. The majority of HAp is available in Nano form, with the remainder available in microform, with Portugal, Japan, and the United States being the primary producers (Dileepkumar et al., 2022).

The purpose of this research is to synthesize HAP powder from a variety of calcium sources, especially simple and easily accessible calcium salts, in diverse morphological forms, and used as adsorbents to remove iron and manganese ions from water sources.

2. Materials and Methods

2.1 Chemicals and Reagents:

Different sources of calcium were used in preparing nano hydroxyapatite materials as following [$CaCl_2$ – Ca $(OH)_2$ – Ca $(CH_3COO)_2$ – Ca $(NO_3)_2$]. Other reagents as phosphorus source H_3PO_4 acid 85 %and NH_4OH were purchased from ALFA and ELNASR Companies. The stock solutions of Fe (III) &Mn (II) were prepared with concentration of 1000 mg/L. The desired pH values of solutions were adjusted by either 0.1 M HCLor 0.1 M NaOH.

2.2 Method for fabricated Hydroxyapatite samples:

The following steps were employed to produce four Hydroxyapatite samples as demonstrated in Figure 1different calcium sources weredissolved in distilled H_2O with stirring to give clear calcium solution. Then, 2 ml of H_3PO_4 (85%) was added slowly with continuously stirring to reach the molar ratio Ca/P of 1.67. After that, the solution of NH_4OH (33%) was added to the above suspension solution until pH value reached 10. The final suspended solution was microwaved for 5 minutes at 170 W for growth of hydroxyapatite crystals. Finally, the Hydroxyapatite was filtered, rinsed in deionized water, and dried overnight at 40 °C.

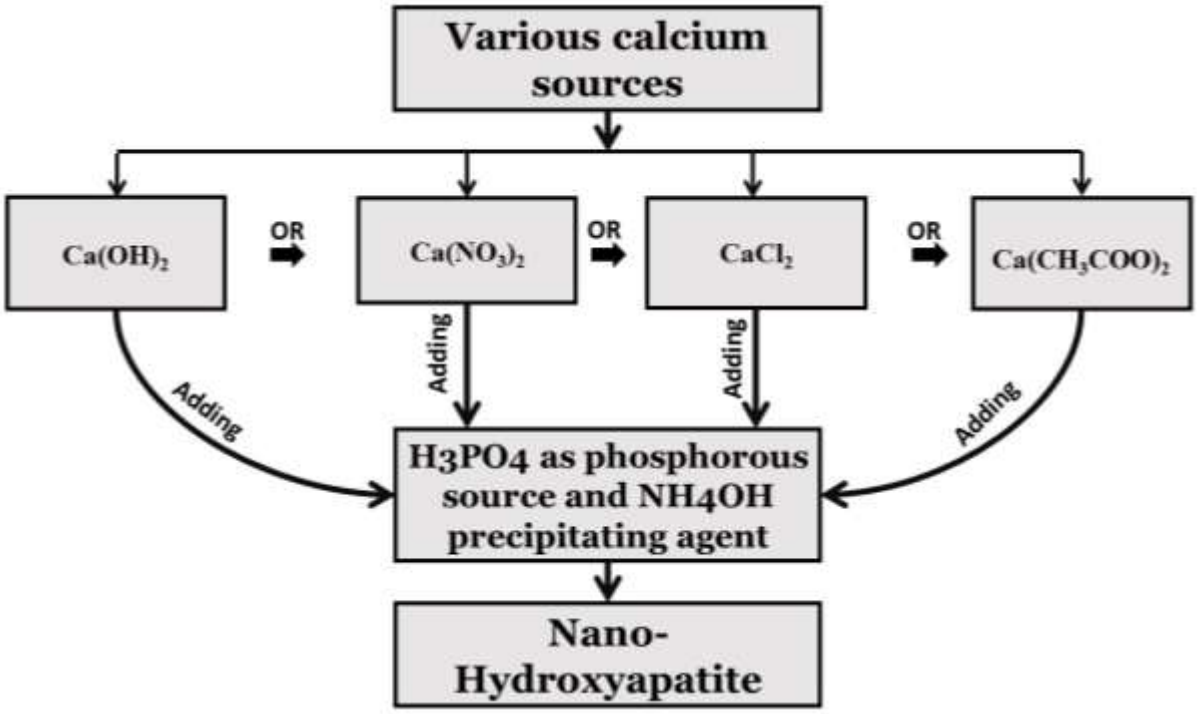

Figure 1: Method for preparation of hydroxyapatite samples.

2.3 Apparatus:

The utilized tools in this research were as following:

- FTIR (Fourier Transform Infrared) measurements (Nicolet) Magna-FTIR – 560 (USA) with KBr technique,
- Powder X-ray Diffraction Analysis (XRD) Brucker Axs-D8- Advance Diffractometer (Belgium) at 2Θ range between 10➡-70➡.
- TG and DSC device model (50H Shimadzu thermal analyzer, Japan).
- Morphology and elemental analysis SEM & EDX (Model FEI INSPECT S50) operating at 20 kV.
- Surface area measurements BET, total pore volume and pore radius using Automatic ASAP 2010 Micrometrics sorptometer (USA) (Quanatachrome Instruments, version 11.04).
- Iron and manganese ions were determined by multiparameter Bench Photometer (Hanna HI -83208) instruments.

3. Result and Discussion

3.1 Mechanism of preparation of hydroxyapatite:

The formation of the hydroxyapatite can be explained using the following simple reactions (Eq. 1)

$10CaX_2.H_2O+5H_2O+20NH_3OH+6H_3PO_4 \rightarrow Ca_{10}(PO_4)6(OH)_2+20NH_4X+15H_2O$ *Equation 1*

$X= Cl^-, OH^-, NO_3^-, CH_3COO^-$

Where X was different anion radical for calcium source as [$CaCl_2$ – Ca $(OH)_2$ – Ca $(CH3COO)_2$ – Ca $(NO_3)_2$]. Based on the findings of the experiments, the following formation mechanism for synthesized HAp might be proposed: The existence of distinct anions throughout

the preparation process act as structural directing agent during the interaction of diverse calcium ions with concentrated phosphoric acid as a source of phosphorous group. Similar trend was reported by others (Sundarabharathi et al., 2019).

3.2. Characterizations of the synthetic Hydroxyapatite:

3.2.1 XR D analysis

The structural information and phase present in the synthesized nanomaterials were investigated using X-ray diffraction (XRD) patterns (Mousa et al., 2013). Figure 2showed the XRD patterns of tested HApsamples. As displayed in Table 1, all prepared hydroxyapatite samples showed hexagonal crystal structures matching card numbers of COD- 9011095, 9010050 and 9011096 for pure phase of hydroxyapatite. Besides, samples showed significant diffraction peaks at 2= 25.8°, 31.4°, 49.4°, and 53.4° identical tohydroxyapatite (Ayash et al., 2019; Cahyaningrum et al., 2018; Encinas-Romero et al., 2013). Aside from the peaks of the HA phase, no additional peaks such as -TCP or -TCP were found, indicating that the produced samples were of high phase purity. The existence of sharp diffraction peaks suggests that the produced samples are crystalline (Sundarabharathi et al., 2019). The crystallite size of the hydroxyapatites analyzed ranged from 14.85 to 25.72 nm, putting it with in Nano scale according to prior studies (Glab et al., 2021; Parhi et al., 2004). The nitrate anion precursors produced the smallest particles size as compared to samples formed from acetate anions. Comparable observation were reported with other researches (Sundarabharathi et al., 2019).

Table 1: Chemical structure, phases, and the crystallite size for Hydroxyapatite sampl**es.**

Sample name	major phase	Chemical structure	JCPDS card	Crystallite size nm
HA – Cl	**Apatite-(CaOH)**	**$Ca_5HO_{13}P_3$**	**COD 9011092**	**16.43**
HA – AC	**Apatite-(CaOH)**	**$Ca_5HO_{13}P_3$**	**COD 9011095**	**25.72**
HA – NO_3	**Apatite-(CaOH)**	**$Ca_5HO_{13}P_3$**	**COD 9011095**	**14.85**
HA – OH	**Apatite-(CaOH)**	**$Ca_5HO_{13}P_3$**	**COD 9011095**	**17.12**

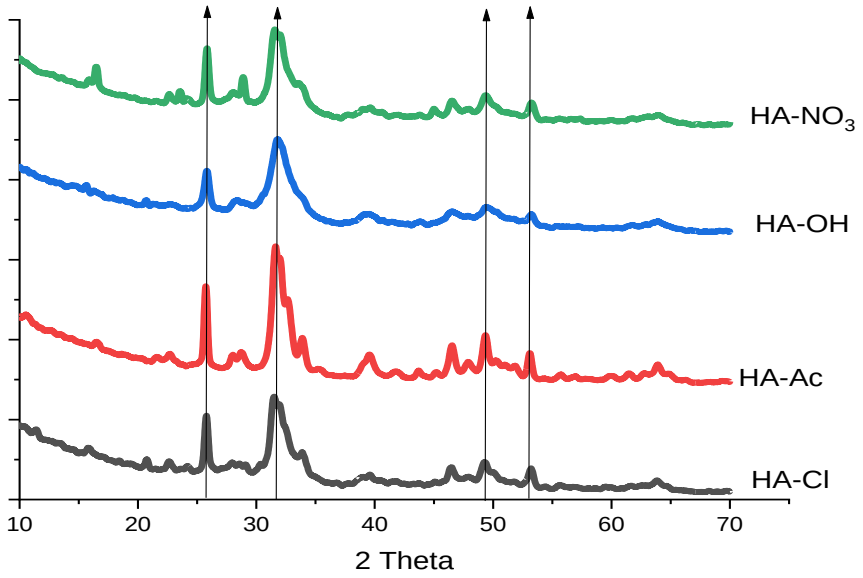

Figure 2: XRD pattern for synthetized hydroxyapatite samples

3.2.2 *FTIR analysis:*

Fourier transform infrared (FTIR) spectroscopy was also used to identify the composition and chemical bonding of HAp (Huang, A. et al., 2019). All FT-IR spectrum were obtained in the range 400–4000 cm^{-1} as presented in Figure 3. The characteristic absorption bands of the phosphate group $(PO_4)^{-3}$in apatite were observed at (1061-1007cm^{-1}, 574–533 cm^{-1}, and 634–607 cm^{-1}. While the H-O-H bands of lattice water showed wide bands in the regions (1600 - 1700 cm^{-1} and 3200 - 3600 cm^{-1}) (Ananth et al., 2018; Ayash et al., 2019). The carbonate (CO_3^{2-}) functional group, which appears at 1405.91 cm^{-1} indicates that the (CO_3^{2-}) group possesses C– O vibration caused by the absorption of atmospheric carbon dioxide during processing(MousaHanna, 2013; Sirait et al., 2020) (Sundarabharathi et al., 2019).

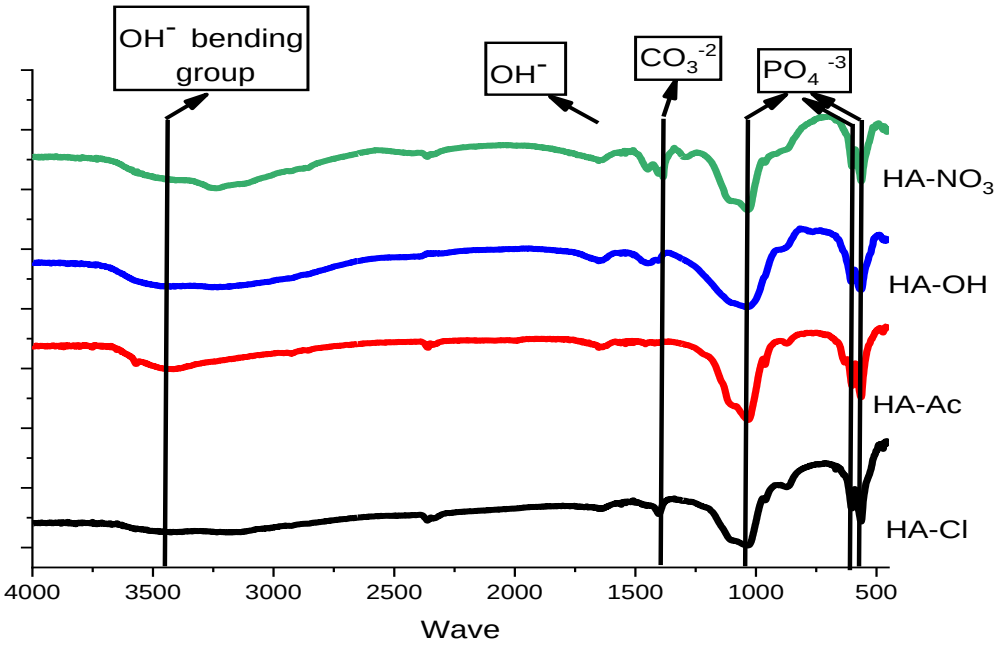

Figure 3: FTIR spectra for fabricated hydroxyapatite samples

3.2.3 SEM analyses:

The structural morphology of HAp nanoparticles generated with diverse anionic precursors was studied using FESEM (Rehman et al., 2016; Sundarabharathi et al., 2019).The morphology and formation of HAp particles were affected by external ionic species presented in the solution, as demonstrated in Fig. 4 (a - d).The inclusion of nitrate in the salt precursor (Fig. 4d) results in a non-uniform nanostructure in the sticks (Sadat-Shojai et al., 2010). Figure 4b shows how HAp made from an acetate precursor sample was molded into Nano sheets and disseminated throughout the structure, self-assembling into flower-like patterns (Zhao, al., 2013, 2014). The sample made from chloride is shaped like coral reefs and contains distinct nanoparticles, as seen in Figure 4a. While, the formation of aggregates in the sample created with the hydroxide precursor results in cotton-shaped nanoparticles, as seen in Figure 4c (Sadat-Shojai et al., 2013)

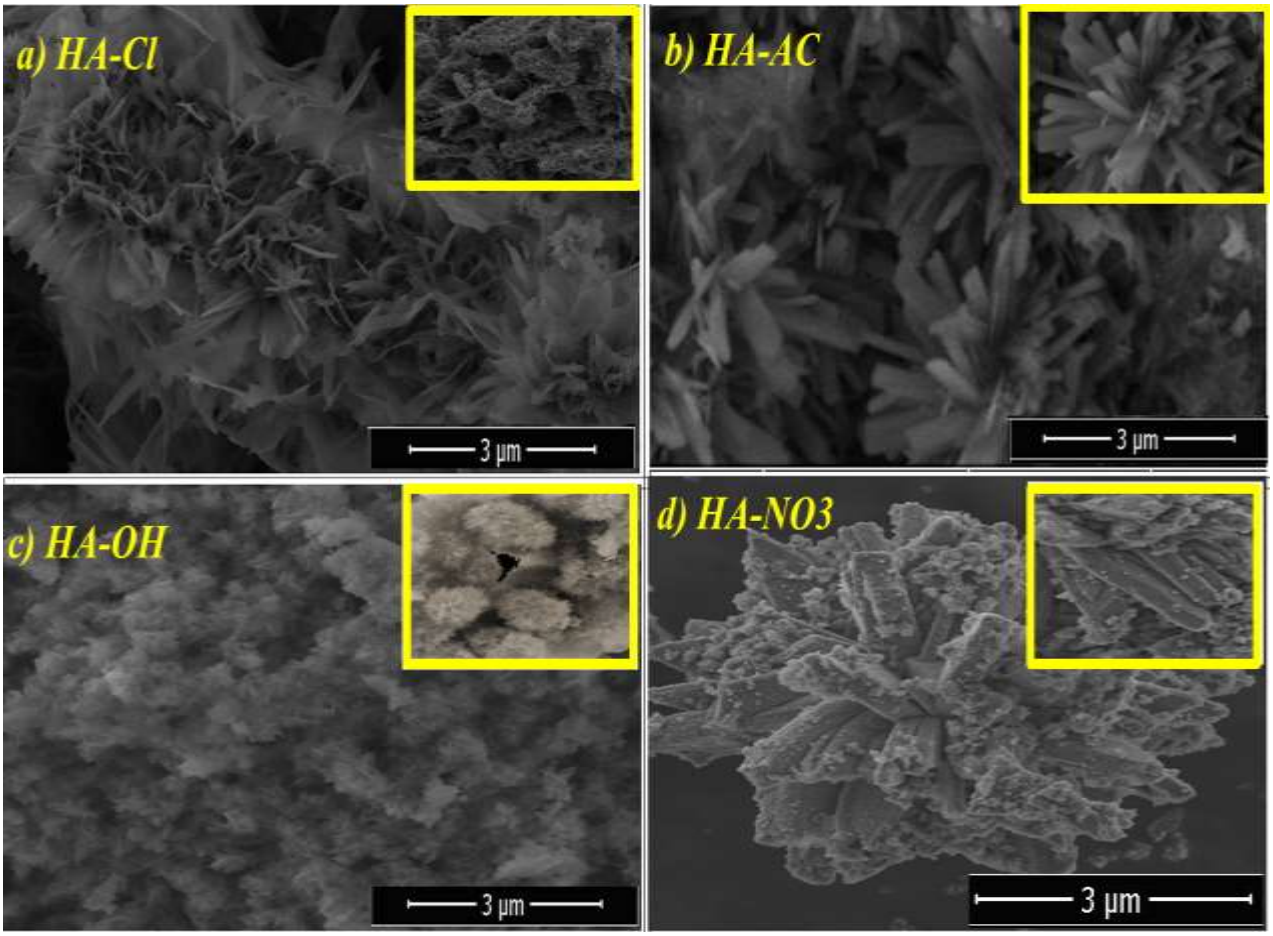

Figure 4: SEM morphology for synthetic hydroxyapatite samples.

3.2.4 ***Surface area measurements:***

The N_2 adsorption-desorption isothermtechnique was used to analyze the surface of the produced HAp nanoparticles (Mondal et al., 2016).Figure 5 (a, b) and Table 2 displayed the data derived from surface area measures such as BET, total pore volume, and average pore radius of the HA samples.All tested sample have high specific surface areas following the order: HA-Cl (162.7 m^2/g)>HA-OH (136.3 m^2/g) >HA-AC (135.3 m^2/g) >HA-NO_3(116 m^2/g).The shape of isotherm between volume of gas adsorbed versus P/P_o revealed type I that characteristics of microporous materials (Huang, L. H. et al., 2019).Type I isotherms have been encountered for microporous materials with tiny external surfaces. Absorption is limited by the available microporous volume rather than the inner surface area (Klobes and Munro, 2006).

Table 2: Surface properties for synthesized hydroxyapatite samples**.**

Sample name	BET square ($m^2.g^{-1}$)	Total pore volume ($cm^3.g^{-1}$)	Aaverage pore radius (Aº)
HA-NO_3	115.98	0.05476	9.44
HA-OH	136.32	0.06999	10.27
HA-AC	135.27	0.06845	10.12
HA-Cl	162.73	0.07220	8.87

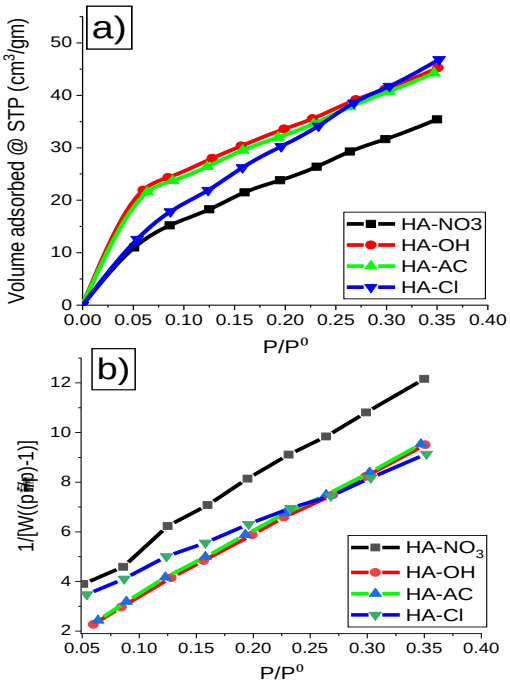

Figure 5: N_2 adsorption isotherms determined at 77.35 K hydroxyapatite samples.

3.2.5. *Thermo-gravimetric analysis:*

TGA is a robust and reliable method for assessing the thermal stability of a substance. TGA, DTG, and DSC curves for hydroxyapatite samples were evaluated in Figure 6 (a-d) for tested hydroxyapatite samples (HA-Cl, HA-AC, HA-NO_3, and HA-OH). Overall weight losses for the studied HAp samples were ranged from1 to 3% demonstrating that they were all thermally stable. The weight losses were at temperature below 100 °C which attributed to the release of adsorbed water on the samples. Furthermore, at temperatures below 115 °C, water in the channels evaporates, resulting TG in a one-step path (Hossein, 2008; Sassoni, 2018). DTG curves verified the information provided from TG curves. HA-NO_3 and HA-AC samples displayed a single DTG peak at 94 ^{o}C and 91 ^{o}C, respectively. WhileHA-Cl and HA-OH samples demonstrated DTG peaks at 330^{o}C and 90 ^{o}C, respectively. Higher temperatures can produce dihydroxylation in apatite samples, which has been recorded at temperatures beyond 700°C (Mousa , 2013; Sofronia et al., 2014).

The DSC curves revealed that all the peaks below 200^{o}C in apatite samples showed exothermic nature owing to evaporated adsorbed water (Zhang et al., 2011). The HA-Cl sample, on the other hand, showed a stronger endothermic peak at 330 ^{o}C.

3.3 Utilization of tested Hydroxyapatite to removeFe^{3+} and Mn^{2+} from water sources

The performance of using hydroxyapatite samples with different morphology to eliminate Fe and Mn ions from various water sources. The water samples hadneutral pH (6.9) andinitialmetal concentration of 100 ppm witha dose of 2 g/L at room temperature. The results displayed in Table 3 High efficiency in removal of Fe ions up to 99.9% while poor removal in case Mn ions (El Kady et al., 2016; Moreno et al., 2010).

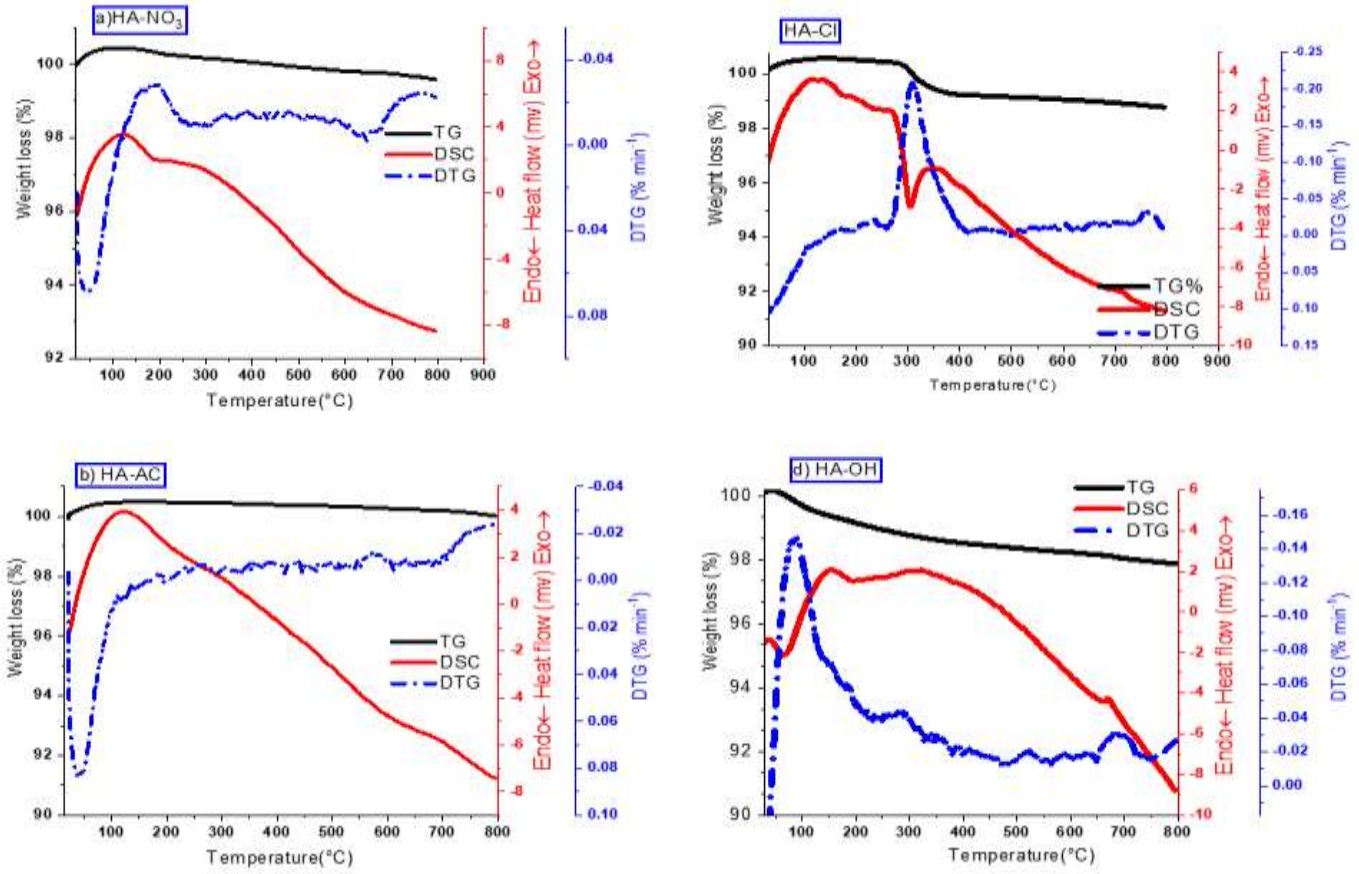

Figure 6: TG, DTG and DSC curves for hydroxyapatite sample

Table 3: Removal of iron and manganese ions from water resource**.**

Sample name	Fe^{3+} Removal %	Mn^{2+} Removal%	pH after Adsorption
HA-NO_3	**99.6%**	**19%**	**5.8**
HA-OH	**99.9%**	**35%**	**6.0**
HA-AC	**99.9%**	**20%**	**5.6**
HA-Cl	**99.8%**	**29%**	**5.7**

3.4 Cost price for manufacturing the nano-hydroxyapatite:

Synthetically produced hydroxyapatite is usually more expensive than non-synthetically produced hydroxyapatite. The market for synthetic-based hydroxyapatite is primarily driven by price growth, reagent costs, and gross revenue. Imagine the challenge that may be posed if diverse Ca sources, such as ($CaCl_2$, Ca $(OH)_2$, Ca $(NO_3)_2$, and Ca $(CH_3COO)_2$, can alter the morphology. In this study, the cost of hydroxyapatite preparation was calculated. Besides, a low-cost technique can be adopted.

The entire expense was due to the energy source employed and the large volume of reagent needed during the hydroxyapatite production. Table (4) displayed the price for manufacturing 100 g of hydroxyapatite. The total cost price was ranged about 258-386 EGP/100g (13.02-19.47) equal €/100g). The HA powder costs were lower than those published by Sigma-Aldrich

company. The powder nano- price of HA (surface area > 80 m^2/g) published from Sigma-Aldrich company were 462 € which equal 9161.9 (EGP) **(Sigma- Aldrich, 2022).**

Table 4: The total cost priceof synthetic nano-HA in this study.

Samples	HA-Cl	HA-NO3	HA-OH	HA-AC	HA®Sigma Aldrich
Cost assessment (EGP) Reagent - chemicals - electricity/100gm	258 (EGP)	386 (EGP)	263 (EGP)	278 (EGP)	9162 (EGP)
Price of HA (€/100 gm)	13.٠٢€	19.47 €	13.27 €	14.02 €	462 €

4. Conclusion

Hydroxyapatite, either biologic or synthetic, is now employed in composites with polymers or other ceramics for bone repair and regeneration, as well as coatings for orthopedic and dental implants. Chemical precipitation may be utilized to manufacture pure HA nanoparticles using a variety of calcium precursor materials. According to XRD data, nano hydroxyapatite has good physical properties, with crystallite sizes ranging from 14 to 25 nm. Furthermore, the artificial HAp materials have anextensive surface area, with BET values ranging from 115 to 162 m^2g^{-1}. Regarding variation calcium sources, the HAp samples displayed a variety of morphological shapes. The weight losses for the HAp samples investigated varied from 1% to 3%, indicating that they were all thermally stable. Iron and manganese ions can easily be removed by HAp as adsorbent from various water sources up to 99.9 % for Fe and 30 % for Mn. When electricity is taken into account, using calcium ions such as $CaCl_2$, $Ca(OH)_2$, $Ca(NO_3)_2$, and $Ca(CH_3COO)_2$ as a calcium source only costs approximately to 258-386 EGP (13.02-19.47 €)/100g.

References

Aldrich, S.2022."Hydroxyapatite". Hydroxyapatite. Retrieved from www.sigma-aldrich.com.

Ananth, K.P., Sun, J.andBai, J. 2018."An innovative approach to manganese-substituted hydroxyapatite coating on zinc oxide(-)coated 316l ss for implant application".Int J Mol Sci, 19(8). doi:10.3390/ijms19082340.

Ayash, A., Abd-El-Aal, M., Elnasr, T.A.S. and Soliman, M.H. 2019."Removing iron ions contaminants from groundwater using modified nano-hydroxyapatite by nano manganese oxide".Journal of Water Resource and Protection, 11(06), 789-809. doi:10.4236/jwarp.2019.116048

Bouyegh, S., Tlili, S., Hassani, M., Mohamed, G.andOussama, B. 2021. Preparation and characteristics of synthesized hydroxyapatite from bovine bones and by co-precipitation method. Paper presented at the International Conference on Industrial Engineering and Operations Management.

Cahyaningrum, S.E., Herdyastuty, N., Devina, B.andSupangat, D. 2018."Synthesis and characterization of hydroxyapatite powder by wet precipitation method".International Conference on Chemistry and Material Science (Ic2ms) 2017, 299. doi:Artn 01203910.1088/1757-899x/299/1/012039.

DileepKumar, V.G., Sridhar, M.S., Aramwit, P., Krut'ko, V.K., Musskaya, O.N., Glazov, I.E. and Reddy, N. 2022."A review on the synthesis and properties of hydroxyapatite for

biomedical applications". J Biomater Sci Polym Ed, 33(2), 229-261. doi:10.1080/09205063.2021.1980985.

El kady, M., Shokry, H.andHamad, H. 2016."Effect of superparamagnetic nanoparticles on the physicochemical properties of nano hydroxyapatite for groundwater treatment: Adsorption mechanism of fe(ii) and mn(ii)", RSC Advances, 6(85), 82244-82259. doi:10.1039/c6ra14497g.

Encinas-Romero, M.A., Peralta-Haley, J., Valenzuela-García, J.L. and Castillón-Barraza, F.F. 2013."Synthesis and structural characterization of hydroxyapatite-wollastonite biocomposites, produced by an alternative sol-gel route".Journal of Biomaterials and Nanobiotechnology, 04(04), 327-333. doi:10.4236/jbnb.2013.44041.

Fihri, A., Len, C., Varma, R.S.andSolhy, A. 2017."Hydroxyapatite: A review of syntheses, structure and applications in heterogeneous catalysis". Coordination Chemistry Reviews, 347, 48-76. doi:10.1016/j.ccr.2017.06.009.

Glab, M., Kudlacik-Kramarczyk, S., Drabczyk, A., Walter, J., Kordyka, A., Godzierz, M., Bogucki, R., Tyliszczak, B.andSobczak-Kupiec, A. 2021."Hydroxyapatite obtained via the wet precipitation method and pvp/pva matrix as components of polymer-ceramic composites for biomedical applications". Molecules, 26(14). doi:10.3390/molecules26144268.

Hossein Eslami, M.S.-H., Mohammadreza Tahriri. 2008."Synthesis and characterization of hydroxyapatite nanocrystals via chemical precipitation technique". Iranian Journal of Pharmaceutical Sciences, SPring 2008: 4(2): 127-134, www.ijps.ir.

Huang, A., Dai, H., Wu, X., Zhao, Z.andWu, Y. 2019."Synthesis and characterization of mesoporous hydroxyapatite powder by microemulsion technique". Journal of Materials Research and Technology, 8(3), 3158-3166. doi:10.1016/j.jmrt.2019.02.025.

Huang, L.H., Sun, X.Y.andOuyang, J.M. 2019."Shape-dependent toxicity and mineralization of hydroxyapatite nanoparticles in a7r5 aortic smooth muscle cells". Sci Rep, 9(1), 18979. doi:10.1038/s41598-019-55428-9.

Ibrahim, M., Labaki, M., Giraudon, J.M.andLamonier, J.F. 2020."Hydroxyapatite, a multifunctional material for air, water and soil pollution control: A review".J Hazard Mater, 383, 121139. doi:10.1016/j.jhazmat.2019.121139.

Klobes, P. and Munro, R. 2006, Porosity and Specific Surface Area Measurements for Solid Materials, Special Publication (NIST SP), National Institute of Standards and Technology, Gaithersburg, MD, [online], https://tsapps.nist.gov/publication/get_pdf.cfm?pub_id=854263 (Accessed June 28, 2022).

Mondal, S., Dey, A.andPal, U. 2016."Low temperature wet-chemical synthesis of spherical hydroxyapatite nanoparticles and their in situ cytotoxicity study".Advances in nano research, 4(4), 295-307. doi:10.12989/anr.2016.4.4.295.

Moreno, J.C., Gómez, R.andGiraldo, L. 2010."Removal of mn, fe, ni and cu ions from wastewater using cow bone charcoal". Materials, 3(1), 452-466. doi:10.3390/ma3010452.

Mousa, S.andHanna, A. 2013."Synthesis of nano-crystalline hydroxyapatite and ammonium sulfate from phosphogypsum waste". Materials Research Bulletin, 48(2), 823-828. doi:10.1016/j.materresbull.2012.11.067.

Munir, M.U., Salman, S., Ihsan, A. and Elsaman, T. 2022."Synthesis, characterization, functionalization and bio-applications of hydroxyapatite nanomaterials: An overview".Int J Nanomedicine, 17, 1903-1925. doi:10.2147/IJN.S360670.

Parhi, P., Ramanan, A.andRay, A.R. 2004."A convenient route for the synthesis of hydroxyapatite through a novel microwave-mediated metathesis reaction". Materials Letters, 58(27-28), 3610-3612. doi:10.1016/j.matlet.2004.06.056.

Rehman, S., Khan, K., Mujahid, M.andNosheen, S. 2016."Synthesis of nano-hydroxyapatite and its rapid mediated surface functionalization by silane coupling agent". Mater Sci Eng C Mater Biol Appl, 58, 675-681. doi:10.1016/j.msec.2015.09.014.

Sadat-Shojai, M., Atai, M., Nodehi, A.andKhanlar, L.N.2010."Hydroxyapatite nanorods as novel fillers for improving the properties of dental adhesives: Synthesis and application". Dent Mater, 26(5), 471-482. doi:10.1016/j.dental.2010.01.005.

Sadat-Shojai, M., Khorasani, M.T., Dinpanah-Khoshdargi, E.andJamshidi, A. 2013."Synthesis methods for nanosized hydroxyapatite with diverse structures". Acta Biomater, 9(8), 7591-7621. doi:10.1016/j.actbio.2013.04.012.

Sassoni, E. 2018."Hydroxyapatite and other calcium phosphates for the conservation of cultural heritage: A review". Materials (Basel), 11(4). doi:10.3390/ma11040557.

Sirait, M., Sinulingga, K., Siregar, N. and Damanik, Y.F. 2020."Synthesis and characterization of hydroxyapatite from broiler eggshell".Paper presented at the 1 The 1st International Conference On Physics And Applied Physics (THE 1St ICP&AP) 2019: Fundamental and Innovative Research for Improving Competitive Dignified Nation and Industrial Revolution 4.0.

Sofronia, A.M., Baies, R., Anghel, E.M., Marinescu, C.A. and Tanasescu, S. 2014."Thermal and structural characterization of synthetic and natural nanocrystalline hydroxyapatite". Mater Sci Eng C Mater Biol Appl, 43, 153-163. doi:10.1016/j.msec.2014.07.023.

Sundarabharathi, L., Ponnamma, D., Parangusan, H., Chinnaswamy, M.andAl-Maadeed, M.A.A.2019."Effect of anions on the structural, morphological and dielectric properties of hydrothermally synthesized hydroxyapatite nanoparticles".SN Applied Sciences, 2(1). doi:10.1007/s42452-019-1807-3.

Zhang, H. and Zhang, M.2011."Characterization and thermal behavior of calcium deficient hydroxyapatite whiskers with various ca/p ratios".Materials Chemistry and Physics, 126(3), 642-648. doi:10.1016/j.matchemphys.2010.12.067.

Zhao, X.-Y., Zhu, Y.-J., Chen, F., Lu, B.-Q.and Wu, J. 2013."Nanosheet-assembled hierarchical nanostructures of hydroxyapatite: Surfactant-free microwave-hydrothermal rapid synthesis, protein/DNA adsorption and ph-controlled release".CrystEngComm, 15(1), 206-212. doi:10.1039/c2ce26315g.

Zhao, X.Y., Zhu, Y.J., Zhao, J., Lu, B.Q., Chen, F., Qi, C. and Wu, J. 2014."Hydroxyapatite nanosheet-assembled microspheres: Hemoglobin-templated synthesis and adsorption for heavy metal ions".J Colloid Interface Sci, 416, 11-18. doi:10.1016/j.jcis.2013.10.034.